SPECTRAL BRIGHTNESS AND RADIUS OF THE ADJACENCY EFFECT FOR OBSERVATION MADE THROUGH THE ATMOSPHERE

I.Yu. Makushkina and V.V. Belov

Institute of Atmospheric Optics,
Siberian Branch of the Academy of Sciences of the USSR, Tomsk
Received September 6, 1990

Results of investigations of the adjacency effect in observations made through the gas–aerosol atmosphere are discussed. The analysis is based on a numerical experiments which make use of the Monte–Carlo method and single scattering approximation.

As is well known, the adjacency effect is one source of light noise in image transfer through scattering media. In contrast to haze, which arises only when the underlying surface is illuminated by an external source, the adjacency effect also appears when a self–illuminated image plane is observed. This noise results in distortion of the true spatial structure of the image of the object so that this structure can be completely destroyed. Thus study of the adjacency effect is very important for solving the problems of prediction and correction of images obtained from spaceborne platforms. A review of the relevant publications has shown that despite the great interest in this problem, many important aspects of it have still received only insufficient study. In particular, with regard to the spectral behavior of the adjacency effect, the influence of the viewing geometry, etc. In this paper we present a summary of the results of an investigation of the adjacency effect in the Earth's gas–aerosol atmosphere. Moreover, this paper can be considered as a continuation of the work done in Refs. 1 and 2, where an analysis of the formation of the adjacency effect under model conditions, simulating the operation of an actual laboratory setup,[3] was presented.

We chose a mean–cyclic model of the continental aerosol as the model of the atmosphere for our numerical experiments.[4] The molecular component of the atmosphere was taken into account using the data on the scattering and extinction coefficients for mid–latitudes in winter published of R.A. McClatchy, et al.[5] Selective absorption by gases in the atmospheric transparency windows can be taken into account, if necessary, using the model described in Ref. 6 for the meteorological visibility range S_M = 23 km. A significant number of the results were obtained for a cloudless atmosphere; however, in order to establish the trends in the variation of the regularities of formation of the adjacency effect under conditions in which optically thick formations appear in the atmosphere, in many of the numerical experiments we introduce a layer of continuous cloudiness whose scattering phase function corresponds to *C. 1* cloud model and other parameters to the stratus model: geometric thickness Δl = 300 m and extinction coefficient σ_e = 17 km^{-1}. The geometry of the calculations takes into account the sphericity of the Earth's surface and atmosphere. The direction of observation **n** is specified by the zenith angle $0° \le \Theta \le 85°$. The altitude of the observation point above the Earth's surface is taken to be L = 90 km. The underlying surface is assumed to be homogeneous and Lambertian.

The formation of the adjacency effect was analyzed numerically using the BESM–6 computer and the "El'brus" computer system in the single scattering approximation (SAA) and by the Monte–Carlo method. In the latter case the well–known modification of conjugate trajectories was used. A description of the algorithms can be found in Ref. 7.

In the study of the integral characteristics of the adjacency effect two characteristics are usually considered[8–11]: brightness and horizontal dimension (radius) of the adjacency effect. It should be noted that certain differences in the interpretation of these characteristics which occur in the literature does not alter the qualitative behavior of these parameters as functions of optical–geometric conditions of observation. The symbols η_∞ and R_ε (Refs. 1, 2, and 7), which we use for the brightness and radius of the adjacency effect, respectively, are uniquely related to the definitions of other authors. Recall that

$$\eta_\infty(\mathbf{n}) = \int_{-\infty}^{\infty}\int h(x, y; \mathbf{n})\, dx dy ,$$

where $h(x, y; \mathbf{n})$ is the point spread function of the vision system under consideration. The radius R_ε is found from the relation

$$0 < \int_{-R}^{R}\int_{-R}^{R} h(x, y; \mathbf{n}) dx dy / \eta_\infty = \varepsilon \le 1 ,$$

where ε is the specified relative magnitude of the adjacency effect.

Studies have shown that both the magnitude of the adjacency effect and its radius are complicated functions of many variables. They are determined by the optical and geometric conditions of observation as well as by the brightness distribution of the investigated object. Both characteristics of the adjacency effect strongly depend on the albedo of the underlying surface. Let us analyze in detail each of these characteristics.

One of the parameters determining the magnitude of the adjacency effect is the wavelength λ. As was mentioned in Refs. 9 and 10, an increase in λ leads to a decrease in the magnitude of the adjacency effect. However, the results of our calculations have shown that the spectral behavior of this effect is much more complicated. As can be seen from Fig. 1, the decrease of η_∞ with increasing λ is rather a trend replete with nonmonotonic features that depend on the conditions of observation. Such spectral behavior is associated with the simultaneous action of various factors: aerosol (and hence the weighted aerosol + molecular) scattering phase function and atmospheric transmission, various light scattering processes in the real atmosphere, etc.

0235-6880/91/03 218-04 $02.00

These and other factors strongly influence the formation of the adjacency effect. In particular, Fig. 2 illustrates the dependence of η_∞ on the light scattering processes involved —molecular and aerosol. It can be seen from this figure that a qualitatively different spectral behavior of η_∞ is characteristic of these two different light scattering processes. It should be noted in addition, that relative contributions of these processes vary with the altitude. This, in turn, results in additional variations in the weighted scattering phase function as well as in the photon survival probability Λ. According to the estimates of the authors of Refs. 8, 12, and 13, who investigated the effect of Λ on the magnitude of the adjacency effect, this parameter is one of the decisive characteristics determining the value η_∞.

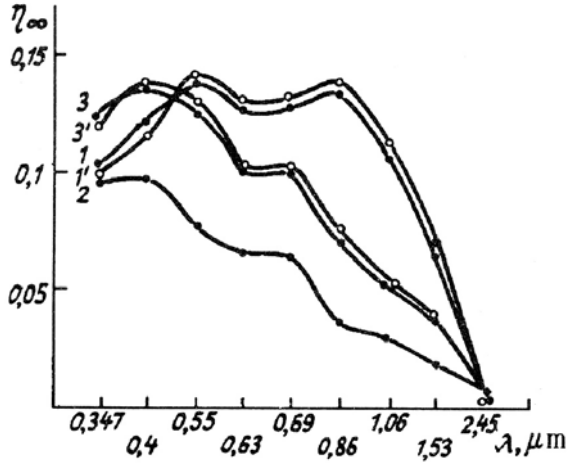

FIG. 1. Spectral behavior of η_∞ at $\Theta = 0°$ (curves 1 and 1'), $\Theta = 30°$ (curve 2), and $\Theta = 70°$ (curves 3 and 3'). Curves 1, 2, and 3 show the results of calculations which take atmospheric sphericity into account; curves 1' and 3' — show the results without atmospheric sphericity.

In addition to the above optical characteristics (λ, Λ, and the aerosol–to–molecular scattering ratio), which have an appreciable effect on the magnitude of the adjacency effect, the effect of the optical thickness τ of the atmospheric vertical column should also be mentioned. According to the results of our calculations and the estimates of other authors,[8,9,12,14] the magnitude of η_∞ is directly proportional to z. As was noted in Ref. 2, the influence of the optical thickness varies qualitatively if a sufficiently wide range of τ values is considered (at least, up to $\tau \approx 12$). In particular, at $\tau \approx 3$ η_∞ has a maximum. Thus, the direct proportionality of $\eta_\infty(\tau)$ is quite realistic if we take into account the fact that the optical thickness of the cloudless atmosphere for the considered spectral ranges usually does not exceed unity.

Let us now consider the influence of the geometry of observation (i.e., the zenith observation angle Θ and the geometric model of the atmosphere and underlying surface) on η_∞. The trends in the behavior of η_∞ as a function of Θ are shown in Figs. 1 and 3 and Table I.

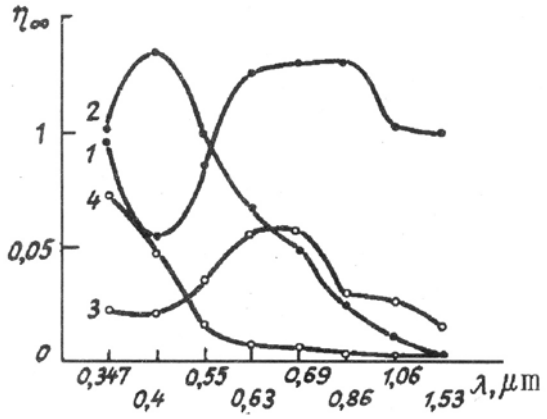

FIG. 2. Spectral dependence of η_∞: 1 and 2 — the results of calculations for $\Theta = 35°$, 3 and 4 — for $\Theta = 0°$. Curves 1 and 3 correspond to aerosol extinction; curves 2 and 4 — the molecular extinction.

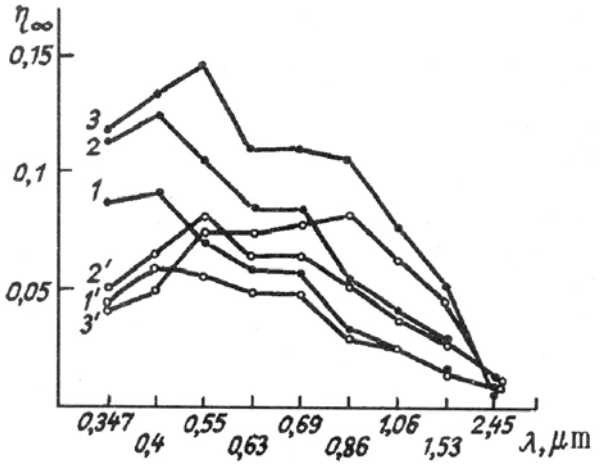

FIG. 3. Spectral dependence of η_∞: 1) $\Theta = 0°$; 2) $\Theta = 60°$; 3) $\Theta = 80°$. Curves 1 — 3 were calculated taking multiple light scattering into account, while curves 1' — 3' were calculated in the single scattering approximation.

TABLE I. Brightness of the adjacency effect η_∞.

λ, μm	Θ, deg.					
	0	30	60	70	80	85
0.347	0.0869	0.0944	0.115	0.122	0.116	0.102
0.4	0.0903	0.0965	0.123	0.135	0.138	0.120
0.55	0.0705	0.0768	0.106	0.125	0.145	0.140
0.69	0.0577	0.0631	0.0839	0.992	0.120	0.129
0.86	0.0308	0.0357	0.0554	0.0707	0.105	0.133
1.06	0.0263	0.0293	0.0417	0.0520	0.0760	0.106
1.53	0.0162	0.0185	0.0289	0.0376	0.0535	0.0641
2.45	0.0101	0.0107	0.0125	0.0116	0.0061	0.0025

As can be seen from these data, the effect of an increase in Θ depends on the wavelength. The behavior of the functions $\eta_\infty^\lambda(\Theta)$ also tends to be affected by the variation of the optical thickness τ with increase of Θ. As was mentioned above, the function $\eta_\infty(\tau)$ has a maximum at $\tau \approx 3$. By comparing the

behavior of η_∞ and τ with increase of Θ, we find that: if the optical thickness of the atmosphere exceeds the value $\tau \approx 3$ at some zenith angle from the considered range $0° \le \Theta \le 85°$, then the function $\eta_\infty(\Theta)$ is nonmonotonic and reaches its maximum just at that angle Θ at which $\tau \approx 3$. And if τ never reaches this value ($\tau < 3$), then the brightness η_∞ increases monotonically with increase of Θ. An exception is the wavelength $\lambda = 2.45$ μm. In this case the function $\eta_\infty(\Theta)$ also reaches a maximum at the angle Θ_{max}, at which the value of the optical thickness is equal to 0.956. This can be explained by the fact that at $\lambda = 2.45$ μm the optical thickness of the atmosphere is due for the most part (in comparison with other wavelengths) to the molecular absorption of light. Therefore, the photon survival probability at this wavelength is lower and, in addition, its value varies with altitude. Such a decrease in Λ results in a shift of the $\eta_\infty(\tau)$ maximum toward the smaller values of τ (this result has also been established by solving the model problem). This fact explains the shift of the $\eta_\infty(\Theta)$ maximum.

The influence of the geometric model is illustrated by Fig. 1. As can be seen from this figure, an account of the sphericity of the atmosphere and the underlying surface has practically no effect on the magnitude of the adjacency effect. A much more substantial difference (not only quantitative but also qualitative) appears when comparing the magnitudes of η_∞ obtained in the single scattering approximation and taking multiple scattering into account. This conclusion is also confirmed by the results shown in Fig. 3. It can be seen from this figure that the error into calculations of the brightness of the adjacency effect in the single scattering approximation can be as high as 50%, even for observations made in the nadir direction. As can be seen from Fig. 3, the accuracy of calculations in the single scattering approximation improves with increase of the wavelength. Of course, some other optical characteristics can also contribute significantly to the error. Generally speaking, the influence of other parameters interacts: a change in one parameter is accompanied, as a rule, by changes in other parameters. Therefore, it is difficult to pinpoint any specific reason for any particular feature in the behavior of the quantities under consideration.

Let us now analyze the behavior of the radius of the adjacency effect in the atmosphere. From Fig. 4 it can be seen that its value R_ε decreases with wavelength. In contrast to the integrated brightness, the function $R_\varepsilon(\lambda)$ is smoother, the only nonmonotonic feature being observed in the vicinity of $\lambda = 1.06$ μm. The matter is that the aerosol scattering phase function is less forward–peaked at just this wavelength of all those considered. Its average cosine at this wavelength is $\langle\cos\Theta\rangle_{1.06} = 0.307$. For comparison, the average cosine of the scattering phase function at its strongest elongation–at $\lambda = 0.4$ μm – $\langle\cos\Theta\rangle_{0.4} = 0.479$. As was shown in Ref. 2, in the solution of the model problem, a weakening of the elongation of the scattering phase function is accompanied by an expansion of the zone of the adjacency effect. This circumstance satisfactorily explains a nonmonotonic behavior of R_ε in the spectral region $\lambda = 0.69$–1.53 μm (it should be noted that $\langle\cos\Theta\rangle_{0.69} = 0.367$, $\langle\cos\Theta\rangle_{0.86} = 0.400$, and $\langle\cos\Theta\rangle_{1.53} = 0.394$). It should be emphasized that the decrease, on the whole, of $R_\varepsilon(\lambda)$ is caused by the decrease in the optical thickness with increase of λ, though there are some other factors that determine (but to a lesser degree than τ) the salient features of the formation of the adjacency effect. A similar conclusion can be drawn from an analysis of the dependence of the size of this zone on the viewing geometry. Thus, from Fig. 4 and Table II it follows that an increase in the observation angle Θ, which is accompanied by an increase in the optical thickness, leads to a monotonic increase in the radius of the adjacency effect.

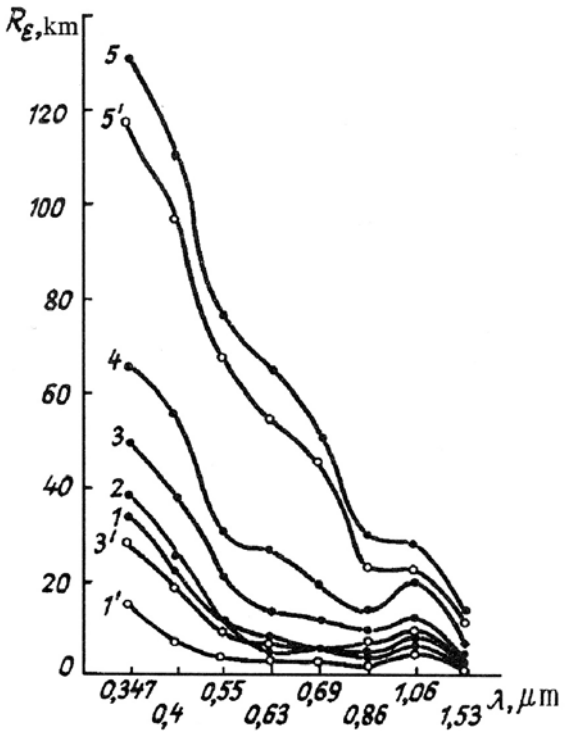

FIG. 4. Spectral behavior of R_ε : $\Theta = 0°$ (curves 1 and 1′), $\Theta = 30°$ (curve 2), $\Theta = 60°$ (curves 3 and 3′), $\Theta = 70°$ (curve 4), and $\Theta = 80°$ (curves 5 and 5′). Curves 1–5 were calculated taking multiple light scattering into account and curves 1′, 3′, and 5′ – in the single scattering approximation. $\varepsilon = 90\%$.

TABLE II. Radius of the adjacency effect R_ε (km). $\varepsilon = 90\%$. *Plane–parallel (upper row) and spherical (lower row) geometric models.*

Θ,	λ, μm						
	0.347	0.4	0.55	0.69	0.86	1.06	1.53
0°	32.5 33	22.5 22	8.5 10	5 5.5	4.5 3.8	6 6	2.3 2.2
60°	162 49	160 38	159.5 21	160 12	160 10	160 12	159 4
85°	969 250	995 220	1158 158	1172 125	1177 73	1175 54	1178 33

At first glance, this fact would seem to contradict the conclusion made in Ref. 2 of the presence of an extremum in $R_\varepsilon(\tau)$ in the range $\tau \le 12$, where in fact a maximum in $R_\varepsilon(\tau)$ is observed at $\tau \approx 6$. In fact, as was mentioned above, a similar conclusion about the behavior of $\eta_\infty(\tau)$, which is based on an analysis of the model problem, also appears to be valid in the case of an aerosol atmosphere. However, it must be stressed that, in

contrast to the integrated magnitude η_∞, the radius of the adjacency effect depends strongly on the distribution of the scattering and extinction coefficients along the observation path (not only on the relative contributions of aerosol and molecular scattering). In addition, according to our estimates and the conclusions derived in Refs. 8 and 14, the radius R_ε depends on the shape of the scattering phase function more strongly than does η_∞. The results shown in Fig. 4 allow one to judge the accuracy of the calculations of R_ε made in the single scattering approximation. As in the case of other characteristics, it can be seen that in the single scattering approximation the calculation error in R_ε is large at the shorter wavelengths and strongly decreases with increase of λ. It should be noted, however, that the single scattering approximation does a better job of describing the qualitative behavior of $R_\varepsilon(\lambda)$ for the considered interval of observation angles than it does of describing the behavior of the magnitude of the adjacency effect.

Let us now analyze the effect of the sphericity of the Earth's surface on R_ε. We shall perform a comparative analysis using the data of Table II, in which some results of calculations of R_ε by the Monte–Carlo method are given.

It is obvious that the necessity of taking into account the sphericity of the Earth's surface is determined by the conditions of observation. Thus, for observations made in the nadir direction the plane–parallel model of the atmosphere provides virtually absolute accuracy, while for larger zenith angles this model leads to great quantitative and qualitative errors. This fact, though unexpected at first glance, can be easily explained. As was already mentioned, the geometry of the model has virtually no effect on the magnitude of the adjacency effect. This is explained by the fact that η_∞ receives contributions from all the radiation arriving from the underlying surface. This being the case, the position of the main zone of formation of the adjacency effect has no great effect. Some small differences appear (because of the difference between the optical thickness of the plane–parallel and spherical models of the atmosphere and an insignificant altitude redistribution of the photon survival probability and the aerosol–to–molecular scattering ratio). The differences in the values of radius of the adjacency effect determined taking and not taking into account the sphericity of the atmosphere are obviously caused by the fundamentally different schemes of formation of the adjacency effect in the two cases. According to our estimates, the presence of a layer of continuous cloudiness increases the integrated magnitude η_∞. As could be expected, vertical displacement of the cloud has practically no effect on the magnitude of η_∞, as can be clearly seen from Table III. Some insignificant differences in η_∞ for different cloud altitudes are associated with small changes in the integral optical thickness of the atmosphere (≈ 0.01) which accompany the cloud movement. As can be seen from the data in Table III, the presence of a cloud has a different effect on the dimension of the adjacency effect zone. The presence of a cloud at low altitudes results in a narrowing of this zone. Lifting the cloud results in an increase of R_ε.

TABLE III. Magnitude and radius of the adjacency effect, $\varepsilon = 95\%$, $\Theta = 0°$, *and* $\lambda = 0.55$ μm.

Parameters	Cloudless atmosphere	Altitude of the cloud		
		250 m	12 km	15 km
η_∞	7.05–02	0.144	0.142	0.143
R, km	19.3	5	47	86

CONCLUSIONS

1. In addition to the albedo of the underlying surface, the main parameters which determine the magnitude and radius of the adjacency effect are the radiation wavelength, the photon survival probability of the aerosol–to–molecular scattering ratio, the optical thickness of the atmosphere, and the direction of observation.

2. Taking account of the sphericity of the Earth's surface and the atmosphere does not influence the results of the calculations of the integral magnitude of the adjacency effect at any angle of observation, but is important when calculating its radius for observations made in directions different from the vertical.

3. Multiple light scattering has a marked effect on the formation of the adjacency effect in the atmosphere in the spectral region $0.347 \le \lambda \le 1.06$ μm and determines its magnitude and radius.

REFERENCES

1. V.V. Belov, B.D. Borisov, V.N. Genin, et al., Izv. Akad. Nauk SSSR, Ser. FAO **23**, No. 11, 1205–1210 (1987).
2. V.V. Belov, B.D. Borisov, and I.Yu. Makushkina, Opt. Atm. **1**, No. 2, 18–24 (1988).
3. B.D. Borisov, V.N. Genin, and M.V. Kabanov, in: *Abstracts of Reports at the 4th All–Union Symposium on Laser Beam Propagation in the Atmosphere*, Tomsk, (1981), Vol. 1, pp. 172–174.
4. G.M. Krekov and R.F. Rakhimov, *Optical Model of Continental Aerosol* (Nauka, Novosibirsk, 1982), 182 pp.
5. R.A. McClatchey, R.W. Fenn, J.E.A. Selby, et al., *Optical Properties of the Atmosphere (Revised)*, Report AFCRL–71–0272 (AFCRL, Bedford, Mass., 1971), 98 pp.
6. S.V. Afonin and A.G. Gendrin, in: *Software for Problems in Atmospheric Optics* (Nauka, Novosibirsk, 1988), pp. 36–65.
7. V.V. Belov and I.Yu. Makushkina, in: *Theory and Applications of Statistical Simulation* (Computer Center of the Siberian Branch of the Academy of Sciences of the USSR, Novosibirsk, 1988), pp. 153–164.
8. J. Otterman and R.S. Fraser, Appl. Opt. **18**, No. 16, 2852–2860 (1979).
9. R.W.L. Thomas, Adv. Space Res. **2**, No. 5, 157–166 (1983).
10. Y.J. Kaufman, J. Geophys. Res. **87**, No. 6, 3165–3172 (1982).
11. R.S. Fraser and Y.J. Kaufman, IEEE Trans. in Geoscience and Remote Sensing **GE–23**, No. 5, 625–633 (1985).
12. Y. Mekler and Y.J. Kaufman, J. Geophys. Res. **85**, No. 7, 4067–4083 (1980).
13. A. Zardecki, S.A.W. Gerstl, and J.F. Embury, Appl. Opt. **23**, 4124–4131 (1984).
14. Y.J. Kaufman and R.S. Fraser, *Invited Paper (A.1.5.1) at the 24th CASPAR Planetary Meeting*, Ottawa, Canada, (1982), pp. 1–19.